HHS Public Access

Author manuscript

Clin Immunol. Author manuscript; available in PMC 2020 August 01.

Published in final edited form as:

Clin Immunol. 2019 August ; 205: 75–82. doi:10.1016/j.clim.2019.06.003.

Silica exposure and chronic virus infection synergistically promote lupus-like systemic autoimmunity in mice with low genetic predisposition

Rosana Gonzalez-Quintial[a], **Jessica M. Mayeux**[b], **Dwight H. Kono**[a], **Argyrios N. Theofilopoulos**[a], **Kenneth M. Pollard**[b], **Roberto Baccala**[a,*]

[a]Department of Immunology and Microbiology, The Scripps Research Institute, La Jolla, CA, USA

[b]Department of Molecular Medicine, The Scripps Research Institute, La Jolla, CA, USA

Abstract

Considerable evidence indicates that autoimmune disease expression depends on both genetic and environmental factors. Among potential environmental triggers, occupational airway exposure to crystalline silica and virus infections have been linked to lupus and other autoimmune diseases in both humans and mouse models. Here, we hypothesized that combined silica and virus exposures synergize and induce autoimmune manifestations more effectively than single exposures to either of these factors, particularly in individuals with low genetic predisposition. Accordingly, infection with the model murine pathogen lymphocytic choriomenigitis virus (LCMV) in early life, followed by airway exposure to crystalline silica in adult life, induced lupus-like autoantibodies to several nuclear self-antigens including chromatin, RNP and Sm, concurrent with kidney lesions, in non-autoimmune C57BL/6 (B6) mice. In contrast, given individually, LCMV or silica were largely ineffectual in this strain. These results support a multihit model of autoimmunity, where exposure to different environmental factors acting on distinct immunostimulatory pathways complements limited genetic predisposition and increases the risk of autoimmunity above a critical threshold.

Keywords

Systemic lupus erythematosus; Autoimmunity; Genetic predisposition; Environmental factors; Crystalline silica; Virus infection

1. Introduction

Systemic autoimmune diseases encompass several disorders with limited therapeutic options and leading to significant health and economic burdens. Systemic lupus erythematosus (SLE), the prototypic systemic autoimmune disease, is characterized by hyperactivation of T

*Corresponding Author: Roberto Baccala, PhD, Department of Immunology and Microbiology, The Scripps Research Institute, 10550 North Torrey Pines Rd, La Jolla, CA 92037, USA, Phone: +1 (858) 784-9920, rbaccala@scripps.edu.

cells, B cells and DCs, and production of autoantibodies to nucleic acids and other associated molecules, leading to immune complex-mediated inflammatory damage in kidneys and other organs [1]. Mechanistically, innate immune pathways of nucleic acid sensing have been implicated in lupus pathogenesis, including activation of endolysosomal Toll-like receptors (TLRs) in B cells and plasmacytoid dendritic cells (pDCs), production of type I interferons (IFN-I), and induction of an IFN-I-dependent gene expression signature [2–6].

Why these innate immune pathways are aberrantly activated in lupus and other autoimmune diseases remains unclear. Genetic factors are clearly crucial for lupus susceptibility, as documented by multiple studies in human SLE [7, 8] and mouse models [9]. However, the low concordance for SLE (<30%) in monozygotic twins [10–13] indicates that, in a significant portion of individuals, the set of inherited predisposing alleles is insufficient, and additional triggers are required for disease expression. Although stochastic events, such as T and B cell antigen receptor generation and epigenetic changes, may contribute to differentiate genetically identical individuals, incomplete concordance for autoimmunity is most likely a reflection of differences in environmental exposures. In fact, lupus and other systemic autoimmune diseases have been associated with several non-genetic factors, most notably silica exposure and virus infections [14–17].

The contribution of crystalline silica to systemic autoimmunity is supported by significant epidemiologic evidence [16, 17]. Silica (silicon dioxide, SiO_2) is one of the most abundant components of rocks, sand and soil. Exposure to respirable crystalline silica is particularly prominent in occupational settings such as mining, construction and other trades, where silica-containing dust is generated by drilling, grinding or cutting [18, 19]. The most common complication of silica inhalation is silicosis, a chronic lung disease characterized by inflammation, tissue damage, and fibrosis [19, 20]. In addition, silicosis is often associated with autoimmune manifestations, sometimes leading to overt disease [21, 22]. Specifically, SLE was found to be ~10 times more prevalent among individuals exposed to high levels of silica than in the general population [18, 21]. Moreover, silica accelerated systemic autoimmunity in lupus-prone mice [23–26], as well as in a fraction of diversity outbred (DO) mice [27], a heterogeneous stock derived from 8 founder strains and maintained by randomized breeding [28–30], but not in non-autoimmune strains such as C57BL/6 (B6) mice [23–26].

Viruses have also been suggested to be important environmental triggers of lupus. The strongest virus/SLE association has been reported for Epstein-Barr virus (EBV), a ubiquitous DNA virus that latently infects ~95% of the human population [31, 32]. EBV promotes B cell proliferation and encodes the EBV nuclear antigen 1 (EBNA1), which may induce *via* mimicry antibodies that crossreact with ribonucleoproteins (RNPs) such as Ro, Sm B/B' and Sm D1, which are typical SLE autoantigens [33–38]. Moreover, recent studies showed that another EBV protein (EBNA2) may participate in allele-dependent formation of transcription complexes at SLE risk loci, potentially leading to disease-related alterations in gene expression programs [39]. In addition to EBV, SLE has been tentatively linked to cytomegalovirus [40], parvovirus B19 [41], and polyomavirus [42]. More directly, the potential contribution of virus infection to systemic autoimmunity has been documented in

animal studies. In this regard, we recently used the lymphocytic choriomeningitis virus (LCMV) in mice with different degrees of predisposition to lupus-like autoimmunity as a model to investigate mechanisms of virus-induced disease acceleration [43]. LCMV was selected because it is one of the best characterized murine viruses, is available in different variants, and can induce either acute or persistent infection depending on the variant and the time of inoculation [44]. In particular, neonatal LCMV inoculation was shown to cause a lifelong persistent infection due to deletion or suppression of virus-specific T cells [45]. We found that a chronic LCMV infection established early in life potently enhanced lupus-like autoantibodies, kidney pathology and mortality in mice with moderate genetic predisposition, but not in non-predisposed B6 mice [43].

These epidemiological and experimental studies provided significant support for the potential role of silica and viruses in systemic autoimmunity, suggesting that these environmental triggers may enhance the risk of disease in individuals with moderate to high genetic predisposition. However, the specific mechanisms of disease exacerbation, and in particular the compound effects of multiple exposures have not been investigated. Here, we hypothesized that silica, viruses, and genetic factors synergize by activating distinct immunostimulatory pathways that together lead to more effective break of tolerance, earlier disease onset, and enhanced severity. We tested this hypothesis in B6 mice, which as mentioned are resistant to autoimmunity induction following exposure to either silica or LCMV [26, 43]. Remarkably, we found that unlike LCMV infection or silica exposure alone, the sequential induction of a persistent LCMV infection early in life followed by silica exposure in adult life induced lupus-like autoantibodies and kidney pathology in this non-autoimmune mouse strain. Thus, this model appears suitable for studies aimed at dissecting mechanisms of synergy between viruses, silica, and genetics in the pathogenesis of systemic autoimmunity.

2. Materials and Methods

2.1. Mice

C57BL/6 (B6) mice (males and females) and BXSB mice (females) were purchased from The Scripps Research Institute Animal Facility or Jackson Laboratory (Bar Harbor, ME) and housed under specific pathogen-free conditions. All experimental protocols were performed according to the NIH Guide for the Care and Use of Laboratory Animals and approved by The Scripps Research Institute Animal Care and Use Committee. Individual mice were randomly assigned to experimental groups and analyzed under identical experimental conditions, but without blinding except for lung and kidney pathological assessments and scoring.

2.2. Virus infection

LCMV Cl13 stocks were prepared by serial passage in BHK-21 cells [46], and purity verified by sequencing [47]. To establish life-long chronic infection, mice were inoculated <24 h after birth using 10^3 plaque-forming units (PFU) per mouse, and serum titers were determined as described [43, 48].

2.3. Silica exposure

Crystalline silica (Min-U-Sil-5, average particle size 1.5–2 μm, U.S. Silica Company, Frederick, MD) was washed in 1 M HCl (2 h at 100°C), rinsed with sterile water, autoclaved (1 h at 121°C), dried, resuspended in PBS and, immediately prior to use, dispersed by sonication [49]. Mice were exposed to a single dose of crystalline silica (5 mg in a total volume of 50 μl of PBS) by transoral (oropharyngeal) instillation as described [27]. The dose used for mouse exposure was calculated based on the National Institute for Occupational Safety and Health (NIOSH) recommendations for human lifetime exposure limit to respirable crystalline silica [26], and a single instillation was applied in consideration of the reported association between the intensity of silica exposure and autoimmunity [18].

2.4. ELISA

Serum levels of polyclonal (total) and anti-chromatin autoantibody IgG were determined by ELISA, using 96-well plates coated with goat anti-mouse immunoglobulin (Jackson ImmunoResearch Laboratories) or chromatin, respectively. Bound antibodies were detected using alkaline phosphatase-conjugated goat anti-mouse IgG (Southern Biotech), and standard curves were generated using calibrated mouse serum (Nordic Immunology). Serum IgG autoantibodies to extractable nuclear antigen 5 (ENA5, encompassing RNP, Sm, SS-A 60 and 52 kDa, SS-B, and Scl-70 antigens), and IgG autoantibodies to RNP and Sm, were analyzed using commercial ELISA kits (QUANTA Lite ELISA Inova Diagnostics, San Diego, CA), which were modified to detect murine samples using horseradish peroxidase-conjugated goat-anti mouse IgG (Thermo Fisher).

2.5. Anti-nuclear autoantibodies

Serum levels of anti-nuclear autoantibodies (ANA) were assessed by incubating HEp-2 slides (Inova Diagnostics, San Diego, CA) with mouse serum diluted 1/100, followed by detection of bound autoantibodies using Alexa-Fluor 488-conjugated goat anti-mouse IgG (Invitrogen). Slides were then mounted using Vectashield Mounting Medium (Vectorlabs, Burlingame, CA) and visualized with an Olympus BH2 microscope. Digital images of ANA patterns were captured using a LEICA DFC 365 FX camera and analyzed using Leica Application Suite AF software (Leica Microsystems, Buffalo Grove, IL). Fluorescence intensity of autoantibody binding to HEp-2 cell nuclei was quantified for each mouse using ImageJ (National Institute of Health).

2.6. Lung pathology

Lungs were excised and fixed for 24 h in zinc formalin. Paraffin-embedding, sectioning (5 μm), and staining (hematoxylin and eosin or trichrome) were done at the Scripps Histology Core. Stained slides were scanned, and images were stored on Slidepath Digital Image Hub (Leica Microsystems). For mice exposed to PBS or silica alone, four of the five lung lobes (superior, middle, inferior, and left) were scored under blinded conditions for the percent of tissue affected by either peribronchitis and perivasculitis or alveolitis, and the average percent values were determined. For mice exposed to LCMV alone or both LCMV and silica, a single lobe per mouse was examined, and the assigned score was directly used for

graph representations. In addition, lungs were scored on a 0 to 4 scale for the levels of lymphocytic infiltration and granuloma, alveolar macrophage proliferation, proteinosis, and fibrosis.

2.7. Kidney pathology

Proteinuria was determined using Albustix strips (Bayer Corporation) and graded semiquantitatively (0 = negative to traces; 1 = 30 mg/dL; 2 = 100 mg/dL; 3 = 300 mg/dL; 4 ≥ 2000 mg/dL). Kidneys were fixed in zinc formalin and sections stained with Periodic Acid-Schiff (PAS). Slide images were scanned and stored on Slidepath Digital Image Hub (Leica Microsystems). The severity of glomerulonephritis (GN) was determined as described [50] by analyzing > 50 representative glomeruli, which were graded blindly on a 0 to 4 scale based on the extent of histopathological features including glomerular cellularity and size, mesangial thickening, inflammatory exudates, capsular adhesion, obliteration of glomerular architecture, PAS-positive deposits, and tubular changes. A score ≥ 2.0 was considered pathologic.

2.8. Data analysis and statistics

Data were analyzed with GraphPad Prism 6 (San Diego, CA). Comparisons of 3–4 experimental groups were performed using one-way ANOVA with Tukey's multiple comparison test. Comparisons of 2 experimental groups were performed using unpaired two-tailed t-test. $p < 0.05$ was considered significant. Hierarchical cluster analysis was done with Cluster 3.0 and Java TreeView, using a relative change value for each phenotype. Briefly, relative change values were calculated using the formula $[(S - S_{AVG}) \div S_{AVG}]$, where S = mouse data point, and S_{AVG} = average of all mouse samples (including PBS controls). A one-dimensional self-organizing map was constructed along each axis, followed by binary, agglomerative, hierarchical clustering using centered correlation similarity metric and a complete linkage clustering method.

3. Results

3.1. Severe lung pathology in B6 mice exposed to LCMV and silica

To investigate potential synergistic effects of silica and viruses in systemic autoimmunity, B6 mice were inoculated with LCMV at birth to establish a chronic infection [43], and then exposed to 5 mg of crystalline silica at the age of 3.5 mo to induce chronic pulmonary inflammation [27]. Control groups included mice that received only LCMV, silica, or PBS. As previously reported [43], neonatal inoculation with LCMV caused a lifelong persistent infection, shown by serum virus titers > 8×10^4 PFU/mL in adult (2–3 mo-old) mice. The magnitude of silica-induced lung inflammation was verified by histopathological analysis at experiment termination, i.e. age 6.5 mo for mice exposed to either PBS or silica, and 8 mo for mice exposed to either LCMV or both LCMV and silica (LCMV+silica). Lungs of silica-exposed mice showed extensive inflammatory cell infiltrates typically associated with silicosis, including lymphocytes, macrophages and neutrophils, in peribronchial and perivascular areas (affecting 28.0 ± 4.9 % of these areas) as well as in alveolar areas (47.8 ± 6.8 %), which were significantly increased compared to PBS controls (0.15 ± 0.07 % in all areas) (Figure 1A). Chronic LCMV infection was also associated with marked peribronchial

and perivascular inflammatory infiltrates (21.4 ± 2.9 %) compared to PBS controls, whereas the increase in alveolar infiltrates (22.0 ± 6.4 %) did not reach statistical significance (Figure 1A). Strikingly, lung pathology was much more severe in mice exposed to LCMV+silica, which showed enhanced peribronchitis and perivasculitis (83.3 ± 4.0 %) and alveolitis (90.0 ± 8.0 %) compared to PBS or LCMV infection alone (Figure 1A). LCMV+silica also induced more severe lung pathology compared to silica alone, although the silica-only group was analyzed at an earlier time point (12 weeks post-silica) than the LCMV+silica group (18 weeks post-silica). Additional features of pulmonary silicosis significantly increased in mice given LCMV+silica compared to LCMV alone were lymphocytic infiltration and granulomas, alveolar macrophage proliferation, proteinosis, and fibrosis (Figure 1B). Thus, LCMV infection and silica exposure promoted severe lung inflammation in B6 mice.

3.2. LCMV and silica synergistically induce lupus-like autoantibodies in B6 mice

To examine the effects of virus and/or silica on autoantibody production, serological analysis was performed on samples obtained at age 6.5 mo (12 weeks post-silica) from B6 mice given PBS, LCMV, silica, or LCMV+silica. Total polyclonal IgG levels were not significantly different between mice exposed to LCMV, silica, or both (Figure 2A). In contrast, IgG antinuclear autoantibodies (ANA) were significantly increased in mice given LCMV+silica, but not in mice given either LCMV or silica alone (Figure 2B). Serum samples were further analyzed for autoantibodies to chromatin and ENA5, a mixture of extractable nuclear self-antigens encompassing RNP, Sm, SS-A, SS-B and Scl-70, which are typically targeted in lupus. IgG anti-chromatin and anti-ENA5 autoantibodies were minimally induced by either LCMV or silica but were significantly elevated following LCMV+silica exposure (Figure 3A-B). Further dissection of the ENA5 specificities showed increases in anti-RNP and anti-Sm autoantibodies in mice exposed to LCMV+silica, but not in mice given LCMV or silica alone (Figure 3C-D). Collectively, these results clearly document a marked synergistic effect of chronic LCMV infection and pulmonary silicosis in eliciting lupus-like autoantibodies in non-autoimmune B6 mice.

3.3. LCMV and silica synergistically promote kidney pathology in B6 mice

To evaluate the impact of silica exposure, virus infection, and the associated autoantibody production on kidney function, levels of proteinuria were monitored at bimonthly intervals. Consistent with earlier studies in this non-autoimmune mouse strain [26, 43], B6 mice given either silica or LCMV showed very low to undetectable levels of proteinuria (≤ 30 mg/dL) up to the age of 6.5 mo, and the same was observed for mice exposed to LCMV+silica despite the high levels of autoantibodies (Figure 4A). As a comparison, the effect of chronic LCMV infection and silica exposure on renal function was examined in female BXSB mice with moderate predisposition to lupus. Unlike male BXSB mice, which spontaneously develop early-onset severe lupus due to a Y chromosome-associated *Tlr7* gene duplication [51, 52], female BXSB mice develop a late-onset mild disease that can be significantly accelerated by chronic LCMV infection [43]. We found that LCMV+silica induced higher levels of proteinuria (≥ 300 mg/dL in 4 of 5 mice) than LCMV alone (≤ 30 mg/dL in 4 of 4 mice) in 5 mo-old female BXSB mice 10 weeks post-silica administration (Figure 4B), which was associated with significant increases in serum IgG anti-chromatin autoantibodies (6.2 ± 1.5 μg/mL in mice given LCMV+silica vs. 0.9 ± 0.4 μg/mL in mice given LCMV

alone, $p<0.01$). To determine whether, with time, progressive silica- induced inflammation and/or chronic virus infection might lead to more pronounced renal dysfunction, B6 mice given LCMV or both LCMV and silica were followed for an additional 6 weeks, up to the age of 8 mo. Even at this advanced time-point, however, proteinuria remained undetectable (Figure 4A).

We next examined whether potential nephritogenic effects of silica and/or LCMV could be more efficiently revealed by histopathological analysis. At the age of 6.5 mo (12 weeks post-silica), kidneys of silica-exposed B6 mice showed no significant increases in glomerulonephritis (GN) scores compared to PBS controls (Figure 4C). In contrast, prominent kidney pathology was observed in 8 mo-old LCMV-infected B6 mice, most of which (4 of 5) exhibited GN scores ≥ 1.8 (Figure 4C). Notably, silica exposure further increased kidney disease severity in LCMV-infected B6 mice, with 5 of 6 mice showing GN scores ≥ 3.0 (Figure 4C).

3.4. Concurrence of autoimmune features in mice exposed to LCMV and silica

Hierarchical clustering analysis was performed to define unbiased relationships between B6 mice exposed to different triggers (silica, LCMV, or LCMV+silica), as well as between autoimmune features (total IgG, ANA, anti-chromatin, anti-ENA5, anti-RNP, anti-Sm, and GN) induced in these mice (Figure 5A). Remarkably, most mice clustered according to treatment, largely consistent with patterns of low autoantibody and GN levels in the silica-only group, low autoantibody but high GN levels in the LCMV-only group, and high autoantibody and GN levels in the LCMV+silica group. As an exception, despite severe lung inflammation (total score 185 out of 200) consistent with effective silica exposure, one mouse of the LCMV+silica group exhibited a high GN score (3.5) but low autoantibody titers, and accordingly this mouse co-clustered with mice of the LCMV-only group (Figure 5A). Overall, no significant differences were noted between female and male B6 mice in these serologic and histopathologic analyses (not shown). Moreover, hierarchical clustering analysis of autoimmune phenotypes identified two main clusters, one including GN, anti-ENA5, and anti-RNP, and the other ANA, anti-chromatin, and anti-Sm (Figure 5A). In contrast, total IgG titers segregated separately, consistent with the observation that this feature was not significantly affected by silica and/or LCMV exposure. As an additional approach to evaluate the concurrence of autoimmune features induced by LCMV and/or silica, for each mouse we calculated an aggregate autoimmunity score, defined here as the sum of the relative change from the average for all the autoimmune phenotypes examined (Figure 5B). This analysis showed significant increases in mice exposed to both LCMV and silica compared to mice exposed to either trigger alone. Together, these results indicate that a persistent LCMV infection can cause significant kidney damage, which is further augmented in association with increased autoantibody production in mice given both LCMV and silica.

4. Discussion

In this study, we examined the impact of multiple environmental exposures on systemic autoimmune disease onset and severity. We used crystalline silica and virus infection as environmental triggers, based on their reported associations with lupus and other systemic

autoimmune diseases. We found that silica airway exposure more efficiently induced lupus-like autoantibodies in mice chronically infected with LCMV than in non-infected mice. Conversely, the autoimmunity-promoting effect of LCMV infection was amplified by silica exposure. These results have significant implications for our understanding of how environmental triggers affect autoimmune disease susceptibility and pathogenesis.

A critical finding of this study was that, in combination, virus infection and silica exposure induced lupus-like disease manifestations in B6 mice with low genetic predisposition, whereas individually these triggers were ineffectual. In contrast, silica exposure alone was sufficient to exacerbate anti-nuclear autoantibody production and kidney pathology in lupus-prone NZM2410 and NZBWF1 mice [23–26], while LCMV infection alone aggravated autoimmune manifestations in predisposed NZB and female BXSB mice [43]. Notably, in female BXSB mice, LCMV infection followed by silica exposure elicited higher autoantibody titers and more severe kidney disease than LCMV infection alone. The additive effects of virus infection and silica exposure suggest that different environmental triggers contribute in non-redundant ways to systemic autoimmunity in specific genetic backgrounds. Interestingly, although the B6 genetic background contributes less susceptibility to lupus than the BXSB genetic background, B6 mice (both females and males) exposed to LCMV +silica exhibited earlier and more severe autoimmunity than unmanipulated female BXSB mice. Thus, studying the synergistic effects of xenobiotics, infections, and susceptibility genes appears crucial to fully understand autoimmune disease pathogenesis and more precisely determine one individual’s risk of developing such conditions.

In addition to increased autoantibody production, combined silica and virus exposures caused more severe lung inflammation than silica or virus alone. Because silica-exposed mice were analyzed at an earlier time-point than dual-exposure mice, it is possible that, given sufficient time, lung pathology induced by silica alone would be as severe as that induced by LCMV and silica together. However, considering that silica induced more severe lung lymphoplasmacytic infiltration and ectopic lymphoid tissue-like structures in autoimmune than in non-autoimmune mice [26], it is possible that the aggravated lung inflammation in mice given LCMV+silica vs. silica alone might be a consequence of enhanced autoimmunity in addition to the extended time of silica exposure. Further studies with fixed virus and/or silica exposure times and mice with deficiencies in genes or cell types essential for autoimmunity will help to clarify this issue.

In most instances, exposure to both LCMV and silica induced severe GN concurrent with high autoantibody levels, suggesting lupus-like immune complex-mediated kidney immunopathology. However, mice that were LCMV-infected but not exposed to silica, as well as one mouse of the dual-exposure group, showed moderate to severe GN despite low autoantibody titers. Although these mice could have developed nephritogenic autoantibody specificities not tested in this study, another possibility is that kidney histopathology was due in part to the direct effect of virus infection and/or immune complex deposits containing viral proteins and specific antibodies.

In our model of multiple environmental exposures, virus infection was induced early after birth to establish lifelong persistence, while silica oropharyngeal aspiration was provoked at

adult age to simulate occupational exposure. Neonatal inoculation with LCMV was previously shown to induce persistent infection of conventional DCs, pDCs, monocytes and macrophages, concurrent with upregulation of MHC and costimulatory molecules, and activation or hyperresponsiveness of T and B cells [43]. The chronicity of these immunostimulatory effects is likely critical for the increased susceptibility to silica- induced autoimmunity in mice with persistent LCMV infection. Another potentially critical factor is the time of infection. Early life represents a window of time that is fundamental for the functional maturation of the immune system and establishment of immunological tolerance [53–58]. Moreover, certain early life infections were shown to significantly affect inflammatory responses later in life, including after the infectious agent has been cleared [59–63]. Accordingly, neonatal LCMV infection may enhance susceptibility to silica-induced autoimmunity by altering normal immune development, tolerance, and/or homeostasis. Therefore, additional investigations comparing the effect of persistent vs. acute infections established at different time-points in life, including after silica administration, will be important to define the temporal requirements of virus and silica exposures for the induction of autoimmune responses. Moreover, this model will allow examination of the effect of other viruses, particularly mouse variants of EBV, cytomegalovirus and polyomavirus, which as mentioned earlier have been linked to human lupus in some reports.

A key question raised by the present study relates to the mechanistic basis of the synergisms between virus and silica in autoimmunity. Considering the essential role of the innate immune system in spontaneous lupus, we hypothesize that virus and silica might contribute by inducing distinct innate immune pathways that, acting in concert, more efficiently promote inflammatory cell activation both in the lungs and systemically, break of tolerance, and autoimmune disease onset and severity. Silica has been reported to induce NLRP3 inflammasome activation and production of the inflammatory cytokines IL-1β and IL-18 in affected lungs [64–72]. Silica also promoted cell death and release of nucleic acids that mediated cGAS-dependent or independent STING activation and production of IFN-I [73]. These pathways were shown to be critical for lung inflammation and silicosis, but their requirement for silica- induced autoimmunity has not been investigated [17]. On the other hand, LCMV-associated viral RNA activates both endolysosomal (TLR-mediated) and cytosolic (MAVS-mediated) pathways of immunostimulation [74–80]. We found that, in the absence of silica, TLR activation is required for LCMV-induced lupus acceleration in predisposed mice [43], but the role of the MAVS-dependent pathway in this model is currently unknown. Further studies using relevant gene-deleted mice will be required to differentiate the contribution of inflammasome activation, cytosolic and endolysosomal nucleic acid sensing, and the induced inflammatory factors in this model of autoimmunity mediated by multifactorial environmental exposures.

In conclusion, the present study provides evidence that a chronic viral infection can significantly enhance the risk of developing autoimmunity following silica exposure and *vice versa*. Thus, susceptibility to lupus, and likely other autoimmune diseases, appears to depend on the additive effects of a sufficient number of genetic and environmental factors to which an individual is progressively exposed throughout life. Future investigations with appropriate mouse models will allow dissection of the complex mechanistic interplays underlying the synergisms between predisposing genes and combinations of environmental

triggers, providing novel perspectives on autoimmune disease pathogenesis and potential therapeutic approaches.

Acknowledgments

Funding

This work was supported by the National Institute of Health (grant numbers AI121525, ES029581, ES029263, AI007244).

References

[1]. Tsokos GC, Systemic lupus erythematosus, N Engl J Med, 365 (2011) 2110–2121. [PubMed: 22129255]

[2]. Ronnblom L, The type I interferon system in the etiopathogenesis of autoimmune diseases, Upsala journal of medical sciences, 116 (2011) 227–237. [PubMed: 22066971]

[3]. Marshak-Rothstein A, Toll-like receptors in systemic autoimmune disease, Nat Rev Immunol, 6 (2006) 823–835. [PubMed: 17063184]

[4]. Crow MK, Type I interferon in the pathogenesis of lupus, J Immunol, 192 (2014) 5459–5468. [PubMed: 24907379]

[5]. Banchereau R, Cepika AM, Banchereau J, Pascual V, Understanding Human Autoimmunity and Autoinflammation Through Transcriptomics, Annu Rev Immunol, 35 (2017) 337–370. [PubMed: 28142321]

[6]. Theofilopoulos AN, Kono DH, Baccala R, The multiple pathways to autoimmunity, Nat Immunol, 18 (2017) 716–724. [PubMed: 28632714]

[7]. Gutierrez-Arcelus M, Rich SS, Raychaudhuri S, Autoimmune diseases - connecting risk alleles with molecular traits of the immune system, Nat Rev Genet, 17 (2016) 160–174. [PubMed: 26907721]

[8]. Chen L, Morris DL, Vyse TJ, Genetic advances in systemic lupus erythematosus: an update, Current opinion in rheumatology, 29 (2017) 423–433. [PubMed: 28509669]

[9]. Morel L, Mapping lupus susceptibility genes in the NZM2410 mouse model, Adv Immunol, 115 (2012) 113–139. [PubMed: 22608257]

[10]. Block SR, Winfield JB, Lockshin MD, D'Angelo WA, Christian CL, Studies of twins with systemic lupus erythematosus. A review of the literature and presentation of 12 additional sets, The American journal of medicine, 59 (1975) 533–552. [PubMed: 1101680]

[11]. Deapen D, Escalante A, Weinrib L, Horwitz D, Bachman B, Roy-Burman P, Walker A, Mack TM, A revised estimate of twin concordance in systemic lupus erythematosus, Arthritis Rheum, 35 (1992) 311–318. [PubMed: 1536669]

[12]. Jarvinen P, Kaprio J, Makitalo R, Koskenvuo M, Aho K, Systemic lupus erythematosus and related systemic diseases in a nationwide twin cohort: an increased prevalence of disease in MZ twins and concordance of disease features, J Intern Med, 231 (1992) 67–72. [PubMed: 1732401]

[13]. Kuo CF, Grainge MJ, Valdes AM, See LC, Luo SF, Yu KH, Zhang W, Doherty M, Familial Aggregation of Systemic Lupus Erythematosus and Coaggregation of Autoimmune Diseases in Affected Families, JAMA Intern Med, 175 (2015) 1518–1526. [PubMed: 26193127]

[14]. Munz C, Lunemann JD, Getts MT, Miller SD, Antiviral immune responses: triggers of or triggered by autoimmunity?, Nat Rev Immunol, 9 (2009) 246–258. [PubMed: 19319143]

[15]. Chervonsky AV, Influence of microbial environment on autoimmunity, Nat Immunol, 11 (2010) 28–35. [PubMed: 20016507]

[16]. Miller FW, Alfredsson L, Costenbader KH, Kamen DL, Nelson LM, Norris JM, De Roos AJ, Epidemiology of environmental exposures and human autoimmune diseases: findings from a National Institute of Environmental Health Sciences Expert Panel Workshop, J Autoimmun, 39 (2012) 259–271. [PubMed: 22739348]

[17]. Pollard KM, Silica, Silicosis, and Autoimmunity, Frontiers in immunology, 7 (2016) 97. [PubMed: 27014276]

[18]. Parks CG, Conrad K, Cooper GS, Occupational exposure to crystalline silica and autoimmune disease, Environ Health Perspect, 107 Suppl 5 (1999) 793–802. [PubMed: 10970168]

[19]. Leung CC, Yu IT, Chen W, Silicosis, Lancet, 379 (2012) 2008–2018. [PubMed: 22534002]

[20]. Kawasaki H, A mechanistic review of silica- induced inhalation toxicity, Inhal Toxicol, 27 (2015) 363–377. [PubMed: 26194035]

[21]. Conrad K, Mehlhorn J, Luthke K, Dorner T, Frank KH, Systemic lupus erythematosus after heavy exposure to quartz dust in uranium mines: clinical and serological characteristics, Lupus, 5 (1996) 62–69. [PubMed: 8646229]

[22]. Conrad K, Mehlhorn J, Diagnostic and prognostic relevance of autoantibodies in uranium miners, Int Arch Allergy Immunol, 123 (2000) 77–91. [PubMed: 11014974]

[23]. Brown JM, Archer AJ, Pfau JC, Holian A, Silica accelerated systemic autoimmune disease in lupus-prone New Zealand mixed mice, Clin Exp Immunol, 131 (2003) 415–421. [PubMed: 12605693]

[24]. Brown JM, Pfau JC, Holian A, Immunoglobulin and lymphocyte responses following silica exposure in New Zealand mixed mice, Inhal Toxicol, 16 (2004) 133–139. [PubMed: 15204774]

[25]. Pfau JC, Brown JM, Holian A, Silica-exposed mice generate autoantibodies to apoptotic cells, Toxicology, 195 (2004) 167–176. [PubMed: 14751672]

[26]. Bates MA, Brandenberger C, Langohr I, Kumagai K, Harkema JR, Holian A, Pestka JJ, Silica Triggers Inflammation and Ectopic Lymphoid Neogenesis in the Lungs in Parallel with Accelerated Onset of Systemic Autoimmunity and Glomerulonephritis in the Lupus-Prone NZBWF1 Mouse, PLoS One, 10 (2015) e0125481. [PubMed: 25978333]

[27]. Mayeux JM, Escalante GM, Christy JM, Pawar RD, Kono DH, Pollard KM, Silicosis and Silica-Induced Autoimmunity in the Diversity Outbred Mouse, Frontiers in immunology, 9 (2018) 874. [PubMed: 29755467]

[28]. Churchill GA, Gatti DM, Munger SC, Svenson KL, The Diversity Outbred mouse population, Mamm Genome, 23 (2012) 713–718. [PubMed: 22892839]

[29]. Svenson KL, Gatti DM, Valdar W, Welsh CE, Cheng R, Chesler EJ, Palmer AA, McMillan L, Churchill GA, High-resolution genetic mapping using the Mouse Diversity outbred population, Genetics, 190 (2012) 437–447. [PubMed: 22345611]

[30]. Logan RW, Robledo RF, Recla JM, Philip VM, Bubier JA, Jay JJ, Harwood C, Wilcox T, Gatti DM, Bult CJ, Churchill GA, Chesler EJ, High-precision genetic mapping of behavioral traits in the diversity outbred mouse population, Genes Brain Behav, 12 (2013) 424–437. [PubMed: 23433259]

[31]. Harley JB, Harley IT, Guthridge JM, James JA, The curiously suspicious: a role for Epstein-Barr virus in lupus, Lupus, 15 (2006) 768–777. [PubMed: 17153849]

[32]. James JA, Robertson JM, Lupus and Epstein-Barr, Current opinion in rheumatology, 24 (2012) 383–388. [PubMed: 22504579]

[33]. Petersen J, Rhodes G, Roudier J, Vaughan JH, Altered immune response to glycine-rich sequences of Epstein-Barr nuclear antigen-1 in patients with rheumatoid arthritis and systemic lupus erythematosus, Arthritis Rheum, 33 (1990) 993–1000. [PubMed: 2164400]

[34]. Sabbatini A, Bombardieri S, Migliorini P, Autoantibodies from patients with systemic lupus erythematosus bind a shared sequence of SmD and Epstein-Barr virus-encoded nuclear antigen EBNA I, Eur J Immunol, 23 (1993) 1146–1152. [PubMed: 8386666]

[35]. McClain MT, Heinlen LD, Dennis GJ, Roebuck J, Harley JB, James JA, Early events in lupus humoral autoimmunity suggest initiation through molecular mimicry, Nat Med, 11 (2005) 85–89. [PubMed: 15619631]

[36]. Chen CJ, Lin KH, Lin SC, Tsai WC, Yen JH, Chang SJ, Lu SN, Liu HW, High prevalence of immunoglobulin A antibody against Epstein-Barr virus capsid antigen in adult patients with lupus with disease flare: case control studies, J Rheumatol, 32 (2005) 44–47. [PubMed: 15630723]

[37]. Poole BD, Scofield RH, Harley JB, James JA, Epstein-Barr virus and molecular mimicry in systemic lupus erythematosus, Autoimmunity, 39 (2006) 63–70. [PubMed: 16455583]

[38]. McClain MT, Poole BD, Bruner BF, Kaufman KM, Harley JB, James JA, An altered immune response to Epstein-Barr nuclear antigen 1 in pediatric systemic lupus erythematosus, Arthritis Rheum, 54 (2006) 360–368. [PubMed: 16385527]

[39]. Harley JB, Chen X, Pujato M, Miller D, Maddox A, Forney C, Magnusen AF, Lynch A, Chetal K, Yukawa M, Barski A, Salomonis N, Kaufman KM, Kottyan LC, Weirauch MT, Transcription factors operate across disease loci, with EBNA2 implicated in autoimmunity, Nat Genet, 50 (2018) 699–707. [PubMed: 29662164]

[40]. Halenius A, Hengel H, Human cytomegalovirus and autoimmune disease, Biomed Res Int, 2014 (2014) 472978. [PubMed: 24967373]

[41]. Pavlovic M, Kats A, Cavallo M, Shoenfeld Y, Clinical and molecular evidence for association of SLE with parvovirus B19, Lupus, 19 (2010) 783–792. [PubMed: 20511275]

[42]. Gupta N, Nguyen CQ, Modica RF, Elder ME, Garin EH, BK viruria and viremia in children with systemic lupus erythematosus, Pediatr Rheumatol Online J, 15 (2017) 21. [PubMed: 28399927]

[43]. Gonzalez-Quintial R, Nguyen A, Kono DH, Oldstone MBA, Theofilopoulos AN, Baccala R, Lupus acceleration by a MAVS-activating RNA virus requires endosomal TLR signaling and host genetic predisposition, PLoS One, 13 (2018) e0203118. [PubMed: 30199535]

[44]. Oldstone MB, Campbell KP, Decoding arenavirus pathogenesis: essential roles for alpha-dystroglycan-virus interactions and the immune response, Virology, 411 (2011) 170–179. [PubMed: 21185048]

[45]. Jamieson BD, Ahmed R, T-cell tolerance: exposure to virus in utero does not cause a permanent deletion of specific T cells, Proc Natl Acad Sci U S A, 85 (1988) 2265–2268. [PubMed: 3258424]

[46]. Borrow P, Evans CF, Oldstone MB, Virus-induced immunosuppression: immune system-mediated destruction of virus-infected dendritic cells results in generalized immune suppression, J Virol, 69 (1995) 1059–1070. [PubMed: 7815484]

[47]. Emonet SF, Garidou L, McGavern DB, de la Torre JC, Generation of recombinant lymphocytic choriomeningitis viruses with trisegmented genomes stably expressing two additional genes of interest, Proc Natl Acad Sci U S A, 106 (2009) 3473–3478. [PubMed: 19208813]

[48]. Ahmed R, Salmi A, Butler LD, Chiller JM, Oldstone MB, Selection of genetic variants of lymphocytic choriomeningitis virus in spleens of persistently infected mice. Role in suppression of cytotoxic T lymphocyte response and viral persistence, J Exp Med, 160 (1984) 521–540. [PubMed: 6332167]

[49]. Hamilton RF Jr., Thakur SA, Mayfair JK, Holian A, MARCO mediates silica uptake and toxicity in alveolar macrophages from C57BL/6 mice, J Biol Chem, 281 (2006) 34218–34226. [PubMed: 16984918]

[50]. Andrews BS, Eisenberg RA, Theofilopoulos AN, Izui S, Wilson CB, McConahey PJ, Murphy ED, Roths JB, Dixon FJ, Spontaneous murine lupus-like syndromes. Clinical and immunopathological manifestations in several strains, J Exp Med, 148 (1978) 1198–1215. [PubMed: 309911]

[51]. Pisitkun P, Deane JA, Difilippantonio MJ, Tarasenko T, Satterthwaite AB, Bolland S, Autoreactive B cell responses to RNA-related antigens due to TLR7 gene duplication, Science, 312 (2006) 1669–1672. [PubMed: 16709748]

[52]. Subramanian S, Tus K, Li QZ, Wang A, Tian XH, Zhou J, Liang C, Bartov G, McDaniel LD, Zhou XJ, Schultz RA, Wakeland EK, A Tlr7 translocation accelerates systemic autoimmunity in murine lupus, Proc Natl Acad Sci U S A, 103 (2006) 9970–9975. [PubMed: 16777955]

[53]. Adkins B, Leclerc C, Marshall-Clarke S, Neonatal adaptive immunity comes of age, Nat Rev Immunol, 4 (2004) 553–564. [PubMed: 15229474]

[54]. PrabhuDas M, Adkins B, Gans H, King C, Levy O, Ramilo O, Siegrist CA, Challenges in infant immunity: implications for responses to infection and vaccines, Nat Immunol, 12 (2011) 189–194. [PubMed: 21321588]

[55]. Dowling DJ, Levy O, Ontogeny of early life immunity, Trends Immunol, 35 (2014) 299–310. [PubMed: 24880460]

[56]. Belnoue E, Fontannaz P, Rochat AF, Tougne C, Bergthaler A, Lambert PH, Pinschewer DD, Siegrist CA, Functional limitations of plasmacytoid dendritic cells limit type I interferon, T cell responses and virus control in early life, PLoS One, 8 (2013) e85302. [PubMed: 24376875]

[57]. Guerau-de-Arellano M, Martinic M, Benoist C, Mathis D, Neonatal tolerance revisited: a perinatal window for Aire control of autoimmunity, J Exp Med, 206 (2009) 1245–1252. [PubMed: 19487417]

[58]. Yang S, Fujikado N, Kolodin D, Benoist C, Mathis D, Immune tolerance. Regulatory T cells generated early in life play a distinct role in maintaining self-tolerance, Science, 348 (2015) 589–594. [PubMed: 25791085]

[59]. Krishnamoorthy N, Khare A, Oriss TB, Raundhal M, Morse C, Yarlagadda M, Wenzel SE, Moore ML, Peebles RS Jr., Ray A, Ray P, Early infection with respiratory syncytial virus impairs regulatory T cell function and increases susceptibility to allergic asthma, Nat Med, 18 (2012) 1525–1530. [PubMed: 22961107]

[60]. Olszak T, An D, Zeissig S, Vera MP, Richter J, Franke A, Glickman JN, Siebert R, Baron RM, Kasper DL, Blumberg RS, Microbial exposure during early life has persistent effects on natural killer T cell function, Science, 336 (2012) 489–493. [PubMed: 22442383]

[61]. Fonseca DM, Hand TW, Han SJ, Gerner MY, Glatman Zaretsky A, Byrd AL, Harrison OJ, Ortiz AM, Quinones M, Trinchieri G, Brenchley JM, Brodsky IE, Germain RN, Randolph GJ, Belkaid Y, Microbiota-Dependent Sequelae of Acute Infection Compromise Tissue-Specific Immunity, Cell, 163 (2015) 354–366. [PubMed: 26451485]

[62]. Bouziat R, Hinterleitner R, Brown JJ, Stencel-Baerenwald JE, Ikizler M, Mayassi T, Meisel M, Kim SM, Discepolo V, Pruijssers AJ, Ernest JD, Iskarpatyoti JA, Costes LM, Lawrence I, Palanski BA, Varma M, Zurenski MA, Khomandiak S, McAllister N, Aravamudhan P, Boehme KW, Hu F, Samsom JN, Reinecker HC, Kupfer SS, Guandalini S, Semrad CE, Abadie V, Khosla C, Barreiro LB, Xavier RJ, Ng A, Dermody TS, Jabri B, Reovirus infection triggers inflammatory responses to dietary antigens and development of celiac disease, Science, 356 (2017) 44–50. [PubMed: 28386004]

[63]. Zhao G, Vatanen T, Droit L, Park A, Kostic AD, Poon TW, Vlamakis H, Siljander H, Harkonen T, Hamalainen AM, Peet A, Tillmann V, Ilonen J, Wang D, Knip M, Xavier RJ, Virgin HW, Intestinal virome changes precede autoimmunity in type I diabetes-susceptible children, Proc Natl Acad Sci U S A, 114 (2017) E6166–E6175. [PubMed: 28696303]

[64]. Srivastava KD, Rom WN, Jagirdar J, Yie TA, Gordon T, Tchou-Wong KM, Crucial role of interleukin-1beta and nitric oxide synthase in silica-induced inflammation and apoptosis in mice, Am J Respir Crit Care Med, 165 (2002) 527–533. [PubMed: 11850347]

[65]. Dostert C, Petrilli V, Van Bruggen R, Steele C, Mossman BT, Tschopp J, Innate immune activation through Nalp3 inflammasome sensing of asbestos and silica, Science, 320 (2008) 674–677. [PubMed: 18403674]

[66]. Cassel SL, Eisenbarth SC, Iyer SS, Sadler JJ, Colegio OR, Tephly LA, Carter AB, Rothman PB, Flavell RA, Sutterwala FS, The Nalp3 inflammasome is essential for the development of silicosis, Proc Natl Acad Sci U S A, 105 (2008) 9035–9040. [PubMed: 18577586]

[67]. Hornung V, Bauernfeind F, Halle A, Samstad EO, Kono H, Rock KL, Fitzgerald KA, Latz E, Silica crystals and aluminum salts activate the NALP3 inflammasome through phagosomal destabilization, Nat Immunol, 9 (2008) 847–856. [PubMed: 18604214]

[68]. Hamilton RF Jr., Thakur SA, Holian A, Silica binding and toxicity in alveolar macrophages, Free Radic Biol Med, 44 (2008) 1246–1258. [PubMed: 18226603]

[69]. Hari A, Zhang Y, Tu Z, Detampel P, Stenner M, Ganguly A, Shi Y, Activation of NLRP3 inflammasome by crystalline structures via cell surface contact, Sci Rep, 4 (2014) 7281. [PubMed: 25445147]

[70]. Biswas R, Hamilton RF Jr., Holian A, Role of lysosomes in silica- induced inflammasome activation and inflammation in absence of MARCO, J Immunol Res, 2014 (2014) 304180. [PubMed: 25054161]

[71]. Tsugita M, Morimoto N, Tashiro M, Kinoshita K, Nakayama M, SR-B1 Is a Silica Receptor that Mediates Canonical Inflammasome Activation, Cell Rep, 18 (2017) 1298–1311. [PubMed: 28147282]

[72]. Giordano G, van den Brule S, Lo Re S, Triqueneaux P, Uwambayinema F, Yakoub Y, Couillin I, Ryffel B, Michiels T, Renauld JC, Lison D, Huaux F, Type I interfero n signaling contributes to chronic inflammation in a murine model of silicosis, Toxicol Sci, 116 (2010) 682–692. [PubMed: 20513754]

[73]. Benmerzoug S, Rose S, Bounab B, Gosset D, Duneau L, Chenuet P, Mollet L, Le Bert M, Lambers C, Geleff S, Roth M, Fauconnier L, Sedda D, Carvalho C, Perche O, Laurenceau D, Ryffel B, Apetoh L, Kiziltunc A, Uslu H, Albez FS, Akgun M, Togbe D, Quesniaux VFJ, STING-dependent sensing of self-DNA drives silica-induced lung inflammation, Nat Commun, 9 (2018) 5226. [PubMed: 30523277]

[74]. Zhou S, Cerny AM, Zacharia A, Fitzgerald KA, Kurt-Jones EA, Finberg RW, Induction and inhibition of type I interferon responses by distinct components of lymphocytic choriomeningitis virus, J Virol, 84 (2010) 9452–9462. [PubMed: 20592086]

[75]. Cervantes-Barragan L, Lewis KL, Firner S, Thiel V, Hugues S, Reith W, Ludewig B, Reizis B, Plasmacytoid dendritic cells control T-cell response to chronic viral infection, Proc Natl Acad Sci U S A, 109 (2012) 3012–3017. [PubMed: 22315415]

[76]. Clingan JM, Ostrow K, Hosiawa KA, Chen ZJ, Matloubian M, Differential roles for RIG-I-like receptors and nucleic acid-sensing TLR pathways in controlling a chronic viral infection, J Immunol, 188 (2012) 4432–4440. [PubMed: 22447976]

[77]. Macal M, Lewis GM, Kunz S, Flavell R, Harker JA, Zuniga EI, Plasmacytoid dendritic cells are productively infected and activated through TLR-7 early after arenavirus infection, Cell Host Microbe, 11 (2012) 617–630. [PubMed: 22704622]

[78]. Walsh KB, Teijaro JR, Zuniga EI, Welch MJ, Fremgen DM, Blackburn SD, von Tiehl KF, Wherry EJ, Flavell RA, Oldstone MB, Toll-like receptor 7 is required for effective adaptive immune responses that prevent persistent virus infection, Cell Host Microbe, 11 (2012) 643–653. [PubMed: 22704624]

[79]. Wang Y, Swiecki M, Cella M, Alber G, Schreiber RD, Gilfillan S, Colonna M, Timing and magnitude of type I interferon responses by distinct sensors impact CD8 T cell exhaustion and chronic viral infection, Cell Host Microbe, 11 (2012) 631–642. [PubMed: 22704623]

[80]. Hervas-Stubbs S, Riezu-Boj JI, Mancheno U, Rueda P, Lopez L, Alignani D, Rodriguez-Garcia E, Thieblemont N, Leclerc C, Conventional but not plasmacytoid dendritic cells foster the systemic virus-induced type I IFN response needed for efficient CD8 T cell priming, J Immunol, 193 (2014) 1151–1161. [PubMed: 24973449]

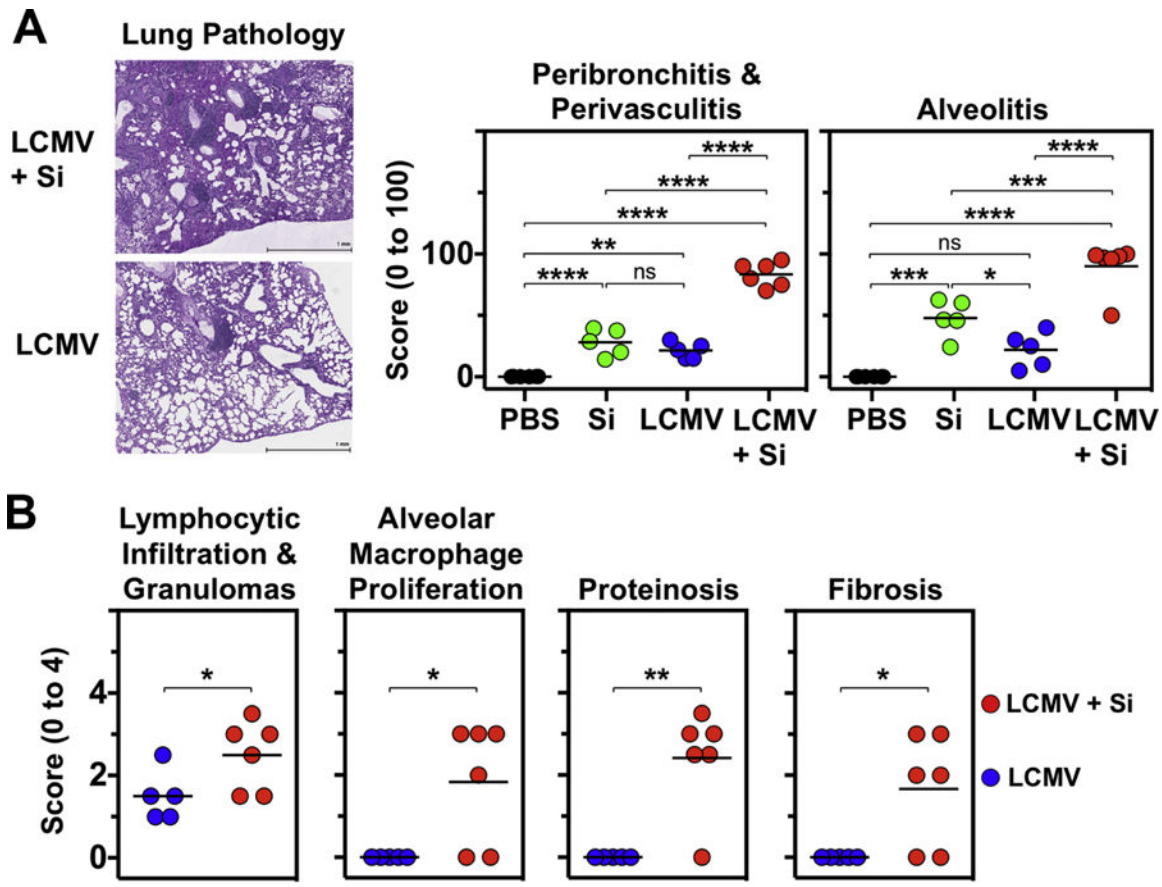

Figure 1.

Severe lung pathology in B6 mice exposed to LCMV and crystalline silica. Mice were infected with LCMV < 24 h after birth and exposed to 5 mg of crystalline silica by oropharyngeal instillation at the age of 3.5 mo. Control mice received LCMV, silica, or PBS alone. Lung pathology was assessed at the age of either 6.5 mo (for mice exposed to either PBS or silica only) or 8 mo (for mice exposed to either LCMV or both LCMV and silica). A) Representative histological sections and lung pathology scores indicating the level of peribronchitis and perivasculitis or alveolitis in each mouse. Data are expressed as percent of affected lung tissue. B) Lung histological sections scored for the levels of lymphocytic infiltration and granuloma, alveolar macrophage proliferation, proteinosis, and fibrosis. Si, silica; dots in graphs, individual mice; horizontal bars, mouse group averages; asterisks, statistical significance (*, $p<0.05$; **, $p<0.01$; ***, $p<0.001$; ****, $p<0.0001$); ns, statistically non-significant.

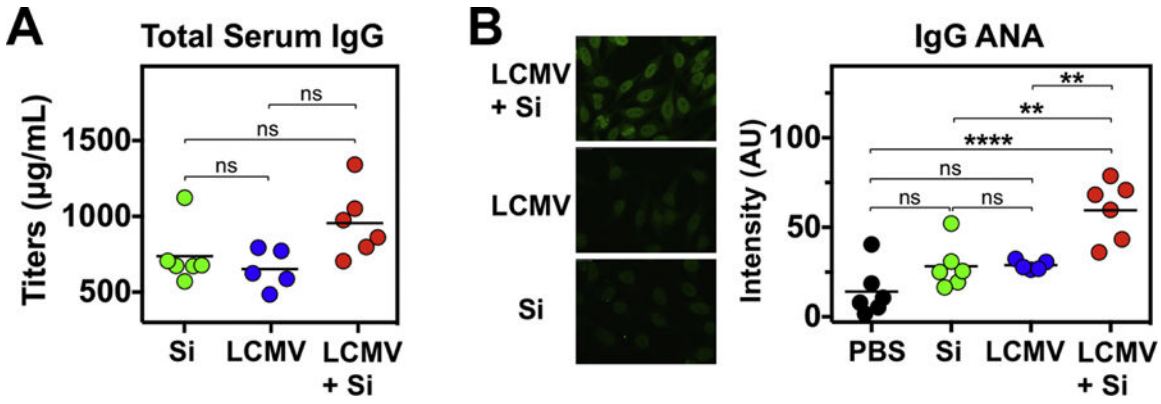

Figure 2.

Combined LCMV and silica exposures induce anti-nuclear autoantibodies in B6 mice. Mice were infected with LCMV < 24 h after birth and exposed to 5 mg of crystalline silica by oropharyngeal instillation at the age of 3.5 mo. Control mice received LCMV, silica, or PBS alone. Serological analysis was performed at the age of 6.5 mo (12 weeks post-silica instillation). A) Total IgG titers determined by ELISA. B) IgG anti-nuclear autoantibody (ANA) titers determined by measuring binding to HEp-2 cell nuclei and immunofluorescence quantification. Data are expressed as percentage of binding compared to a positive control (MRL-lpr mouse serum). Si, silica; AU, arbitrary units; dots in graphs, individual mice; horizontal bars, mouse group averages; asterisks, statistical significance (**, $p<0.01$; ****, $p<0.0001$); ns, statistically non-significant.

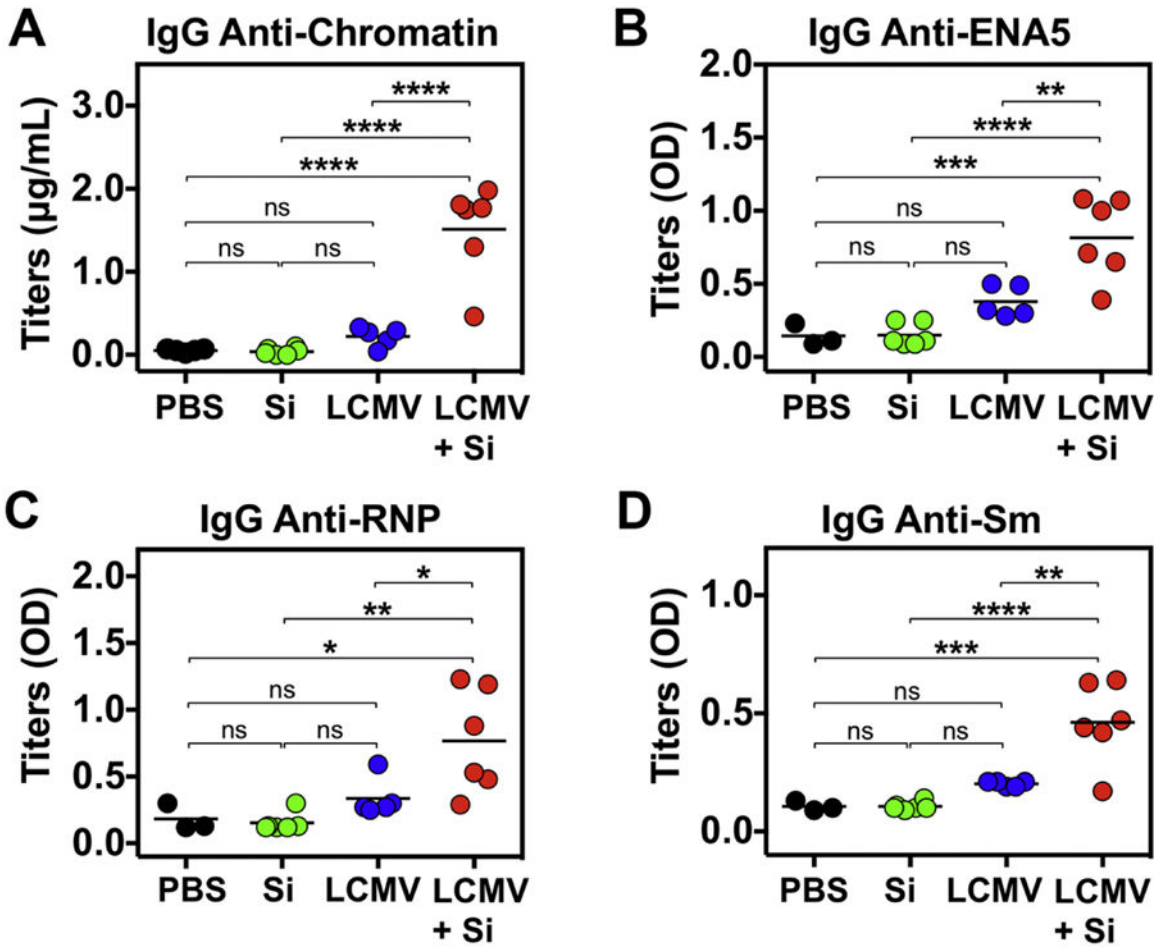

Figure 3.

Combined LCMV and silica exposures induce diverse autoantibodies in B6 mice. Mice were infected with LCMV < 24 h after birth and exposed to 5 mg of crystalline silica by oropharyngeal instillation at the age of 3.5 mo. Control mice received LCMV, silica, or PBS alone. Serological analysis was performed at the age of 6.5 mo (12 weeks post-silica instillation) by ELISA. A) Anti-chromatin IgG autoantibodies. B) Anti-ENA5 (extractable nuclear antigen 5, encompassing RNP, Sm, SS-A 60 and 52 kDa, SS-B, and Scl-70) IgG autoantibodies. C) Anti-RNP (ribonucleoprotein) IgG autoantibodies. D) Anti-Sm (Smith antigen) IgG autoantibodies. Si, silica; OD, optical density; dots in graphs, individual mice; horizontal bars, mouse group averages; asterisks, statistical significance (*, $p<0.05$; **, $p<0.01$; ***, $p<0.001$; ****, $p<0.0001$); ns, statistically non-significant.

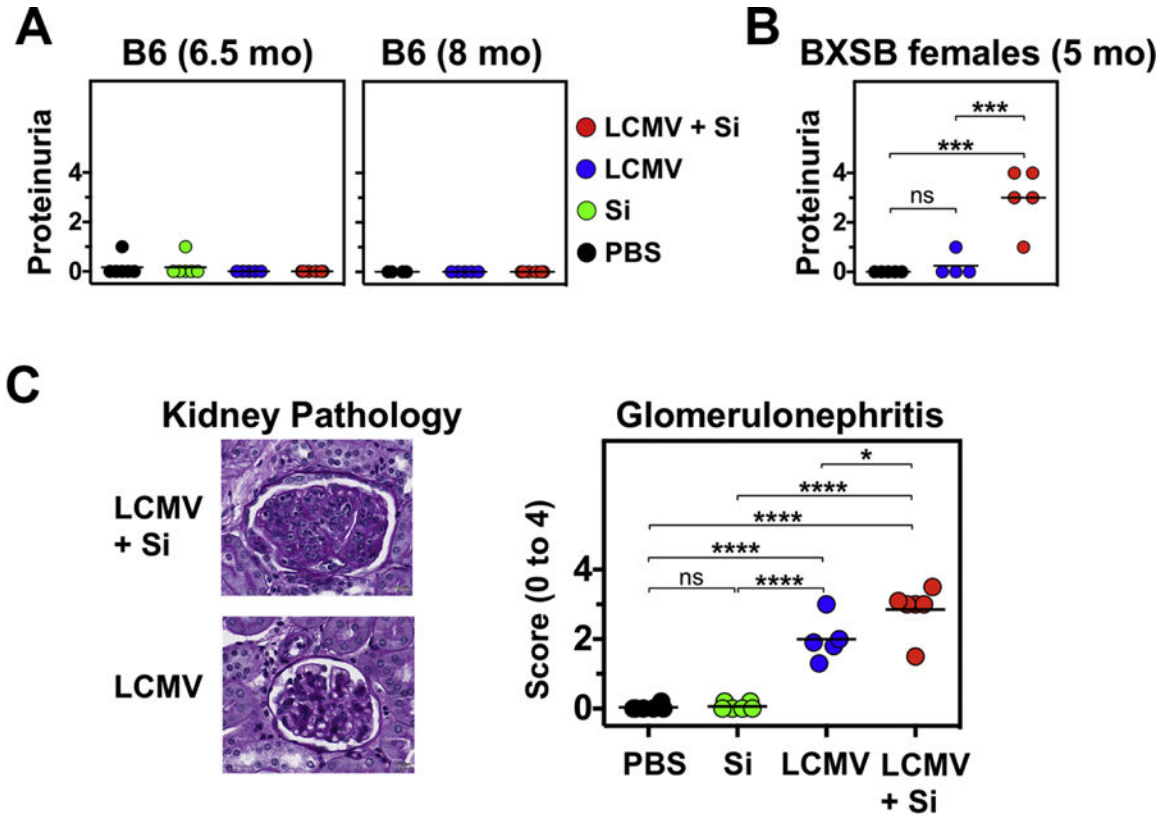

Figure 4.

Combined LCMV and silica exposures induce kidney histopathology in B6 mice. Mice were infected with LCMV < 24 h after birth and exposed to 5 mg of crystalline silica by oropharyngeal instillation at the age of 3.5 mo (B6 mice) or 2.5 mo (female BXSB mice). Control mice received LCMV, silica, or PBS alone. Proteinuria was assessed at the indicated ages, while kidney histological lesions were examined at the age of either 6.5 mo (for mice exposed to either PBS or silica only) or 8 mo (for mice exposed to either LCMV or both LCMV and silica). A) Proteinuria in B6 mice. No significant differences were detected among groups. B) Proteinuria in lupus-predisposed female BXSB mice. C) Kidney histopathological lesions in B6 mice. Representative histological sections and glomerulonephritis (GN) scores for all mice are shown. Si, silica; dots in graphs, individual mice; horizontal bars, mouse group averages; asterisks, statistical significance (*, $p<0.05$; ***, $p<0.001$; ****, $p<0.0001$); ns, statistically non-significant.

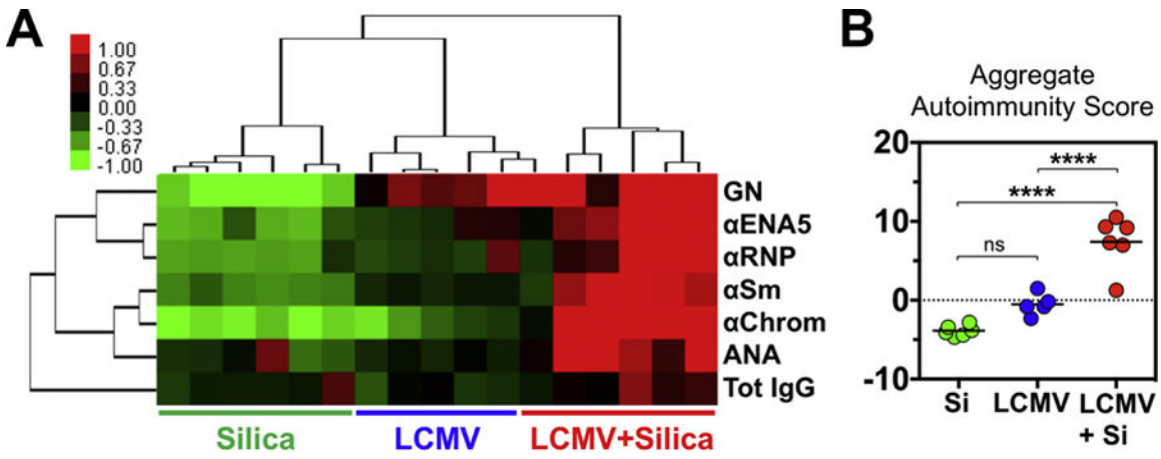

Figure 5.

Concurrence of autoimmune features in B6 mice exposed to both LCMV and silica. Mice were infected with LCMV < 24 h after birth and exposed to 5 mg of crystalline silica by oropharyngeal instillation at the age of 3.5 mo. Control mice received LCMV, silica, or PBS alone. Autoantibody titers were examined as in Figures 2 and 3 at the age of 6.5 mo, while glomerulonephritis (GN) was assessed as in Figure 4 at the age of either 6.5 mo (for mice exposed to either PBS or silica only) or 8 mo (for mice exposed to either LCMV or both LCMV and silica). A) Hierarchical cluster analysis of samples and autoimmune phenotypes. Values are reported as relative changes from the average of all samples (PBS, silica, LCMV, LCMV+silica) and expressed as a heatmap, where red = positive relative change, black = no change, and green = negative relative change. Mice of the PBS-only group are not shown. Each column represents an individual mouse. B) Aggregate autoimmunity score, defined as the sum of all relative changes detected in each mouse. Si, silica; dots in graph, individual mice; horizontal bars, mouse group averages; asterisks, statistical significance (****, $p<0.0001$); ns, statistically non-significant.